Supporting Information

Ultrafast carrier transfer in poly(heptazine imide) for efficient photocatalytic H_2O_2 production: The structure-directing role of in-situ incorporated cations

Shuo Zhang,[a] Jun Yang,[a] Xin Cao,[a] Hui Zhang,*[a] Yuhang Zhao,[a] Yuying Huang,[b] and Jianhua Sun[a]

[a.] *School of Chemistry and Chemical Engineering, Institute of Advanced Functional Materials for Energy, Jiangsu University of Technology, Changzhou 213001, Jiangsu Province, P. R. China.* E-mail: zhanghui@jsut.edu.cn

[b.] *Key Laboratory of Catalysis and Materials Sciences of the State Ethnic Affairs Commission & Ministry of Education, College of Chemistry and Material Science, South-Central Minzu University, Wuhan, 430074, China.*

1. Experimental section

1.1. Synthesis of melon

The traditional carbon nitride with a melon structure (denoted as melon) was prepared by the thermal polycondensation of melamine: 5.0 g melamine was placed into a covered crucible, and then heated at 550℃ for 4 h in a muffle furnace. After cooled to room temperature, the product was ground in a mortar and collected.

1.2. Synthesis of alkali-metal-ion-doped PHIs (K-PHI, NaK-PHI)

Typically, K-PHI was prepared through a molten-salt assisted polycondensation, using LiCl/KCl salts (45/55 wt%, T_m = 352 °C): 1.0 g as-prepared melon and 10 g LiCl/KCl were thoroughly ground. The resulting mixture was transferred into a porcelain crucible and heated in a muffle furnace at 550 ℃ for 4 h. The heating rate was 2.5 ℃·min^{-1}. After cooling to room temperature, the obtained product was washed with hot water several times, collected by filtration and dried at 70 ℃.

NaK-PHI was prepared using a procedure similar to that of K-PHI, except that LiCl/NaCl/KCl salts (33.3/33.3/33.3 wt%, T_m = ~355 °C) was used to replace LiCl/KCl.

1.3. Synthesis of PHI and PHI-2

PHI was obtained by the removal of K from K-PHI: K-PHI (0.5 g) was stirred in 1 M HCl (100 mL) for 1 h at room temperature. The solid product was collected by filtration and washed with water several times, affording a white protonated PHI. For deprotonation, this protonated PHI was then stirred in 1 M $NH_3.H_2O$ (100 mL) for 1 h at room temperature. After filtration, the solid was washed with deionized water until the filtrate was neutral. The resulting pale yellow solid was collected and dried at 70 ℃ to yield the final product, PHI.

PHI-2 was synthesized from NaK-PHI using the same two-step acid/base treatment described above.

1.4. Characterization

X-ray diffraction (XRD) patterns were obtained from a X-Pert Powder X-ray diffractometer (PANalytical). Solid-state ^{13}C NMR measurements were obtained on a Bruker AVANCE NEO 400 spectrometer. X-ray photoelectron spectroscopy (XPS) measurements were conducted on a Thermo Fisher ESCALAB Xi+ spectrometer with

monochromic Al Kα X-ray. Fourier transform infrared spectroscopy (FTIR) spectra were measured on a Thermo Nicolet iS10 spectrometer. UV-vis diffuse reflection spectra (DRS) were recorded on a Perkinelmer Lambda 850+ spectrophotometer. Time-resolved transient photoluminescence spectra were measured on a FluoroMax+ spectrophotometer (HORIBA). Surface potential measurements were conducted on an atomic force microscopy (AFM, SPM-9700) with Kelvin probe.

1.5. Photocatalytic H_2O_2 production

The photocatalytic reduction of O_2 to H_2O_2 was performed in a top-irradiation reaction vessel. Typically, 50 mg of the prepared photocatalyst was dispersed in a mixture of 90 mL deionized water and 10 mL ethanol. The mixture was stirred for 30 min in the dark under continuous O_2 bubbling to reach the absorption-desorption equilibrium. Then the solutions were exposed to visible light provided by a 300 W Xe lamp with a 420 nm cut-off filter (P = 153.8 mW·cm^{-2}, measured by a Newport Oriel 91150V reference cell). A continuous magnetic stirrer and cooling water were applied during the experiment. During the irradiation, ~2 mL solution was sampled every 15 min and filtrated with a 0.45 μm filter to remove the photocatalyst.

The concentration of H_2O_2 was quantified by a colorimetric method using the horseradish peroxidase (HRP)/3,3',5,5'-tetramethylbenzidine (TMB) system. HRP is used to catalyze TMB in the presence of H_2O_2 generating a colored product. Typically, 100 μL of the filtered reaction solution was mixed with 2 mL Na_2HPO_4/NaH_2PO_4 (0.1 M, pH 7.4) buffer, 10 μL TMB (0.1 M), and 10 μL HRP (0.1 M). The mixture turned blue immediately, indicating TMB oxidation. After 10 min, the reaction was quenched by adding 200 μL of H_2SO_4 (3 M), which converted the blue product to yellow for measurement. The concentration of oxidation product formed was quantified spectrophotometrically at 450 nm (The solution was diluted before UV-vis absorption measurement if necessary), from which the concentration of H_2O_2 produced during each reaction was estimated. Fig. S1 shows the linear fitting spectra for the H_2O_2 standard solution.

The apparent quantum efficiency (AQE) for H_2O_2 production was measured by replacing the cut-off filter with corresponding band-pass filter. The AQE is calculated

from the following equation:

$$\text{AQE} = \frac{2 \times \text{number of evolved H2O2 molecules}}{\text{the number of incident photos}} \times 100\%$$

Further, the number of evolved H_2O_2 molecules can be expressed as:

$$\text{the number of evolved } H_2O_2 \text{ molecules} = n(H_2O_2) \cdot N_A$$

And the number of incident photons can be expressed as:

$$\text{the number of incident photons} = \frac{E \times \lambda}{h \times c} = \frac{P \times S \times t \times \lambda}{h \times c}$$

Where $n(H_2O_2)$ refers to the H_2O_2 production (mol), N_A is the Avogadro constant (6.022×10^{23} mol^{-1}); E refers to the total energy of the incident photon (J), λ is the wavelength of incident light (m), h is the Planck constant (6.626×10^{-34} J·s), c is the light speed (3×10^{8} $m\cdot s^{-1}$), P refers to the average spectral irradiance ($W\cdot cm^{-2}$), S is the irradiation area (19.625 cm^2 in this paper), and t is the irradiation time (3600 s in this paper). By integrating above formulas, the AQE is obtained as follows:

$$\text{AQE} = \frac{2 \times n(H_2O_2) \cdot N_A \times h \times c}{P \times S \times t \times \lambda} \times 100\%$$

The measured values of $n(H_2O_2)$ and P are listed in Table S1:

Table S1 The measured data and corresponding AQE

λ / 10^{-9} (m)	$n(H_2O_2)$ / 10^{-6} (mol)	P / 10^{-3} ($W\cdot cm^{-2}$)[a]	AQE (%)
380	135	2.325	51.8
420	148	2.205	54.2
450	322	6.830	35.5
475	73.8	8.500	6.2
500	11.4	4.800	1.6

[a] The average intensity of irradiation was measured by a Newport Oriel 91150V reference cell.

For example, the AQE at 420 nm is calculated as follows:

$$\text{AQE} = \frac{2 \times n(H_2O_2) \cdot N_A \times h \times c}{P \times S \times t \times \lambda} \times 100\%$$

$$= \frac{2 \times 148 \times 10 - 6 \times 6.022 \times 1023 \times 6.626 \times 10 - 34 \times 3 \times 108}{2.205 \times 10 - 3 \times 19.625 \times 3600 \times 420 \times 10 - 9} \times 100\%$$

= 54.2%

1.6. Electrochemical and photoelectrochemical measurements

Electrochemical impedance spectra (EIS), Mott-Schottky plots, and photocurrent responses were measured using a CHI-760E workstation (CH Instruments) in a standard three-electrode system, with the prepared samples as the working electrodes, an Ag/AgCl reference electrode, and a Pt wire counter electrode. For the EIS measurements, a 0.1 M KCl aqueous solution containing 5.0 mM $K_3[Fe(CN)_6]/K_4[Fe(CN)_6]$ (1:1) was used as the electrolyte. Whereas for the photocurrent and Mott-Schottky measurements, a 0.2 M Na_2SO_4 aqueous solution (pH = 6.8) was used as the electrolyte. The working electrodes were prepared as follows: ~5 mg sample was dispersed in 0.02 wt% Nafion solution to afford a suspension. The suspension was sonicated for 1 h and then spread on to a 1.0 cm × 1.0 cm exposed ITO glass, dried in the air. The photocurrent was measured under -0.2 V bias voltage and the light source was a 300 W Xe-lamp with a 420 nm cut-off filter.

2. Figures and Tables

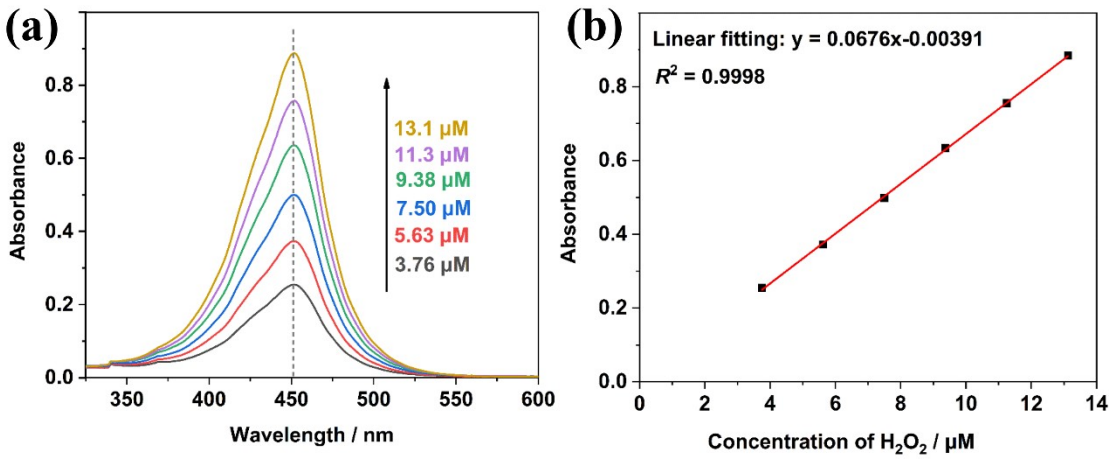

Fig. S1 (a) The standard spectra of the HRP/TMB solution with different concentration of H_2O_2. (b) The corresponding linear fitting: UV-vis absorption intensity at 450 nm vs. concentration of H_2O_2.

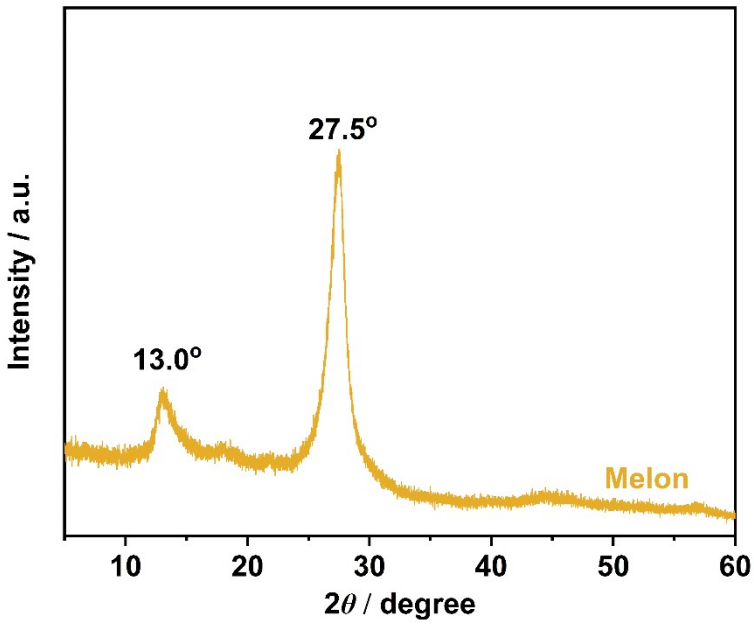

Fig. S2 XRD pattern of melon.

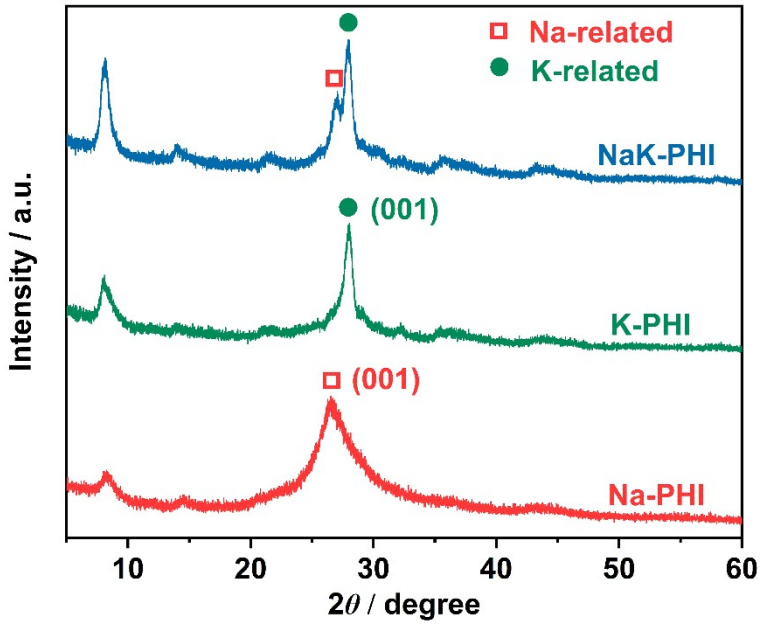

Fig. S3 XRD patterns of Na-PHI, K-PHI, and NaK-PHI. Na-PHI was prepared using a procedure similar to that of K-PHI, except that LiCl/NaCl salts (65/35 wt%, T_m=558 °C) was used to replace LiCl/KCl.

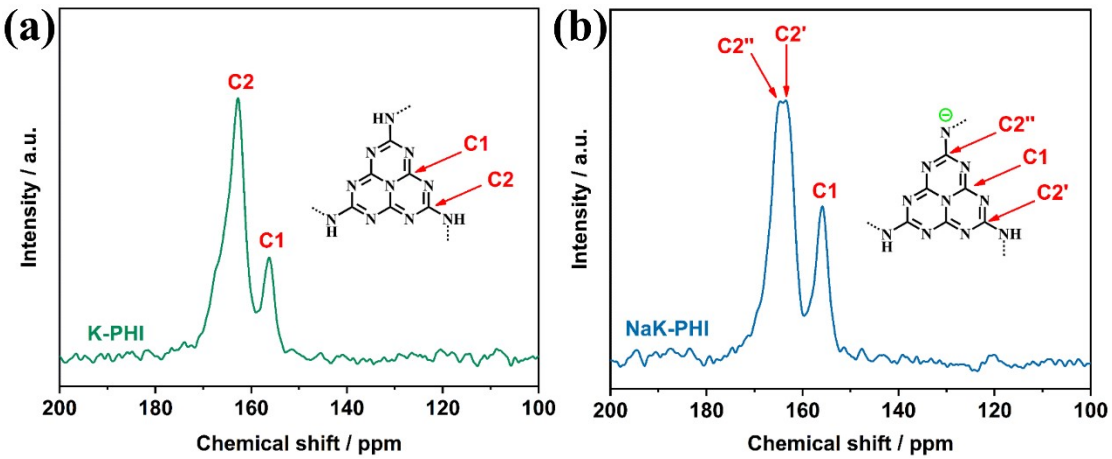

Fig. S4 Solid-state ^{13}C NMR spectra of (a) K-PHI and (b) NaK-PHI.

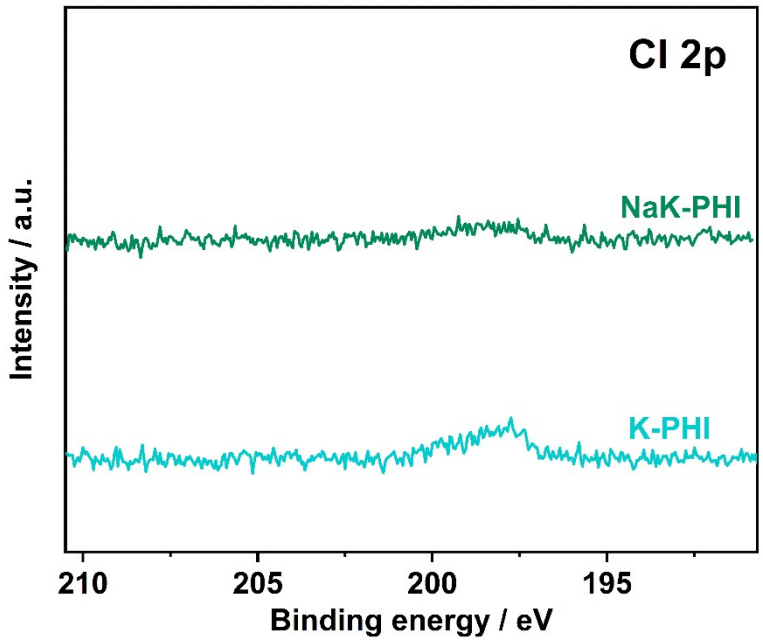

Fig. S5 XPS high-resolution Cl 2p spectra of K-PHI and NaK-PHI.

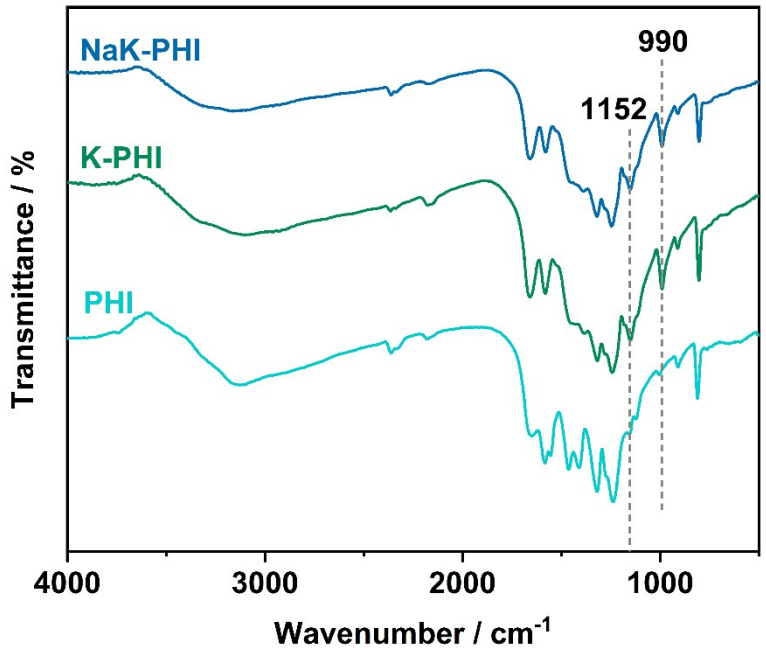

Fig. S6 FTIR spectra of PHI, K-PHI, and NaK-PHI.

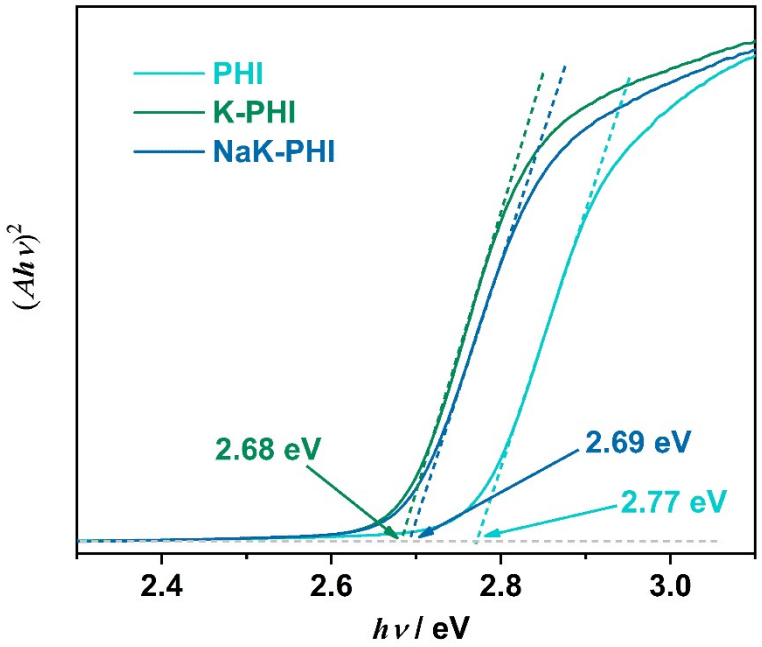

Fig. S7 Tauc plots of PHI, K-PHI, and NaK-PHI.

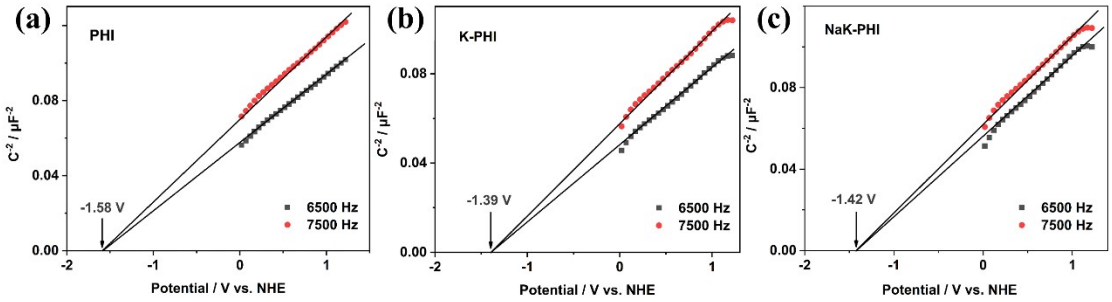

Fig. S8 Mott-Schottky plots of (a) PHI, (b) K-PHI and (c) NaK-PHI. The potentials recorded vs. Ag/AgCl were converted to the NHE scale using the relationship: *E* (vs. NHE) = *E* (vs. Ag/AgCl) + 0.197 V.

Table S2 The fitting parameters of the time-resolved transient photoluminescence decay curves for PHI, K-PHI, and NaK-PHI.

Sample	A_1 / %	τ_1 / ns	A_2 / %	τ_2 / ns	$\tau_{avg.}$ / ns
PHI	84.82	1.53	15.18	14.23	1.77
K-PHI	94.30	1.01	5.70	9.08	1.07
NaK-PHI	74.54	2.76	25.46	23.24	3.56

The emission decay curves of the samples were fitted by biexponential kinetics function (equation 1). The average PL lifetime (τ_{avg}) was deduced by the following equation 2：

$$I(t) = A_1\exp(-t/\tau_1) + A_2\exp(-t/\tau_2) \quad (1)$$

$$\tau_{avg} = \frac{A_1\tau_1^2 + A_2\tau_2^2}{A_1\tau_1 + A_2\tau_2} \quad (2)$$

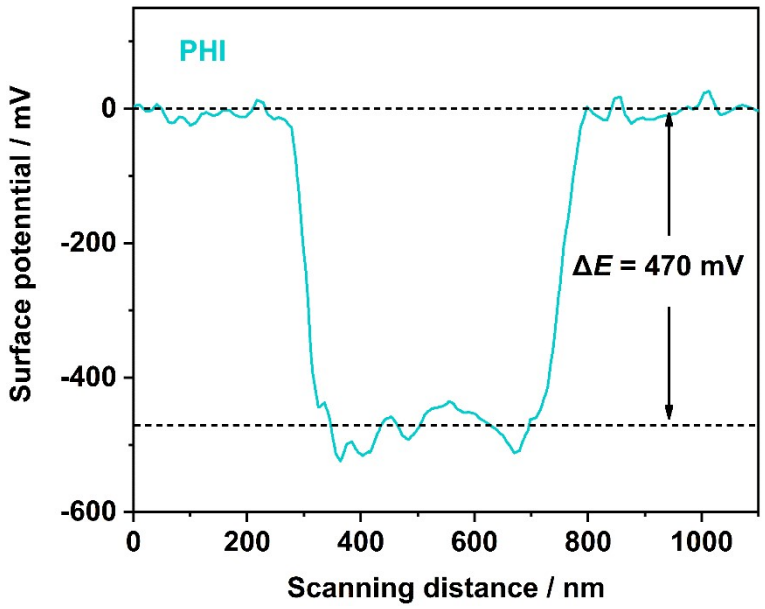

Fig. S9 Linear scanning of the surface potential on PHI along the line marked in Fig. 3e.

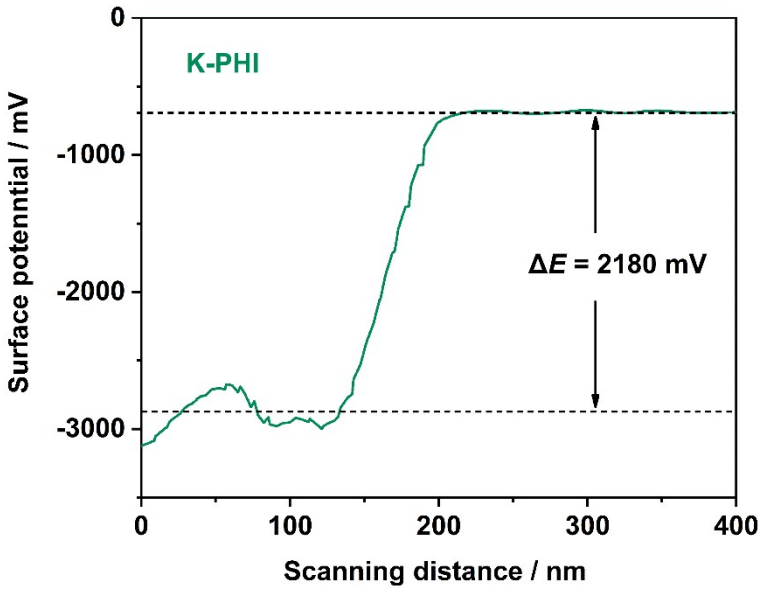

Fig. S10 Linear scanning of the surface potential on K-PHI along the line marked in Fig. 3e.

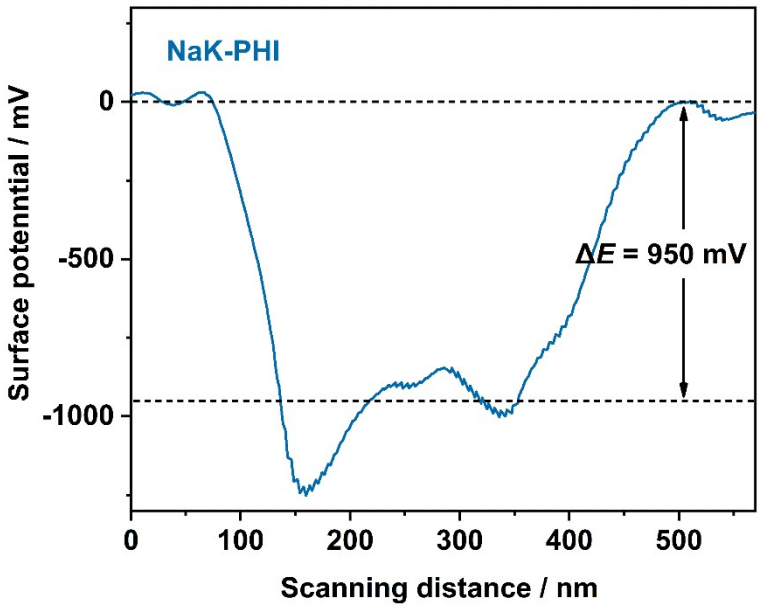

Fig. S11 Linear scanning of the surface potential on NaK-PHI along the line marked in Fig. 3e.

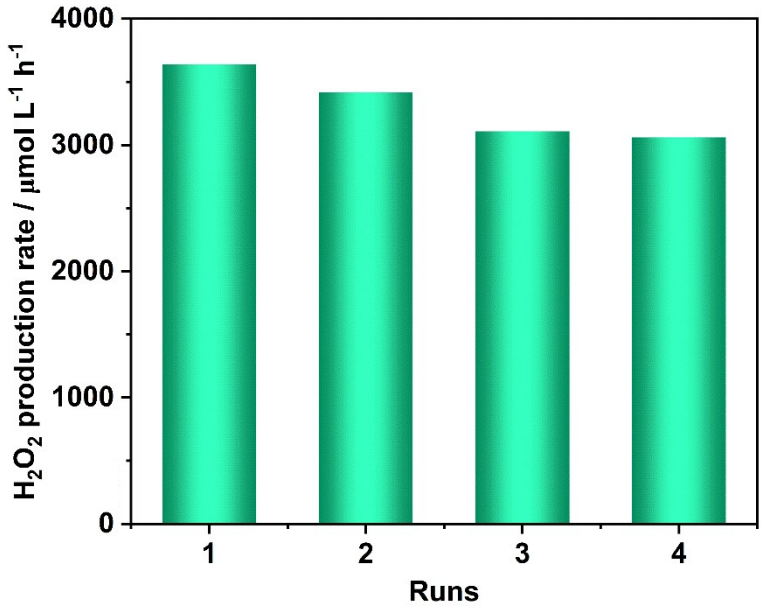

Fig. S12 Cycling test of K-PHI for photocatalytic H_2O_2 production under O_2 atmosphere. Experimental conditions: 50 mg of the catalysts in 100 mL aqueous solutions containing 10 vol% ethanol under visible light (xenon lamp, $\lambda > 420$ nm) irradiation.

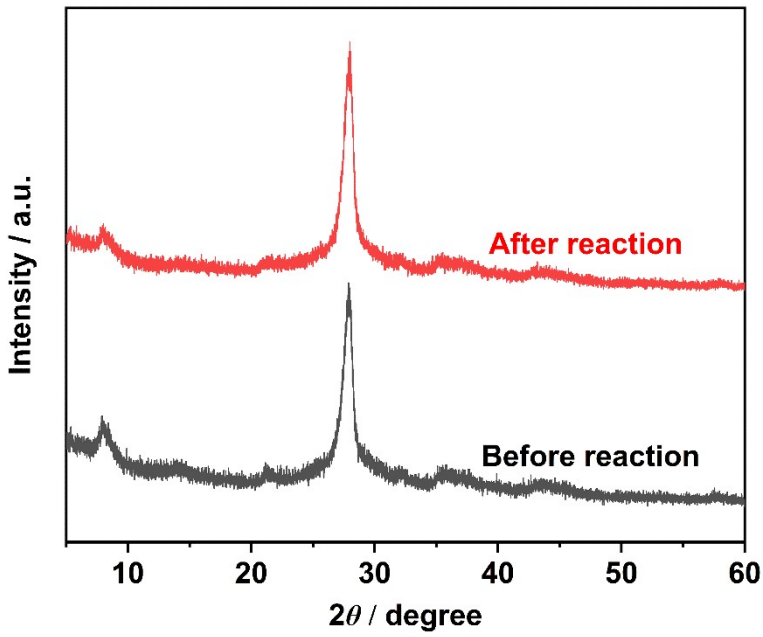

Fig. S13 XRD patterns of K-PHI before and after the photocatalytic reaction.

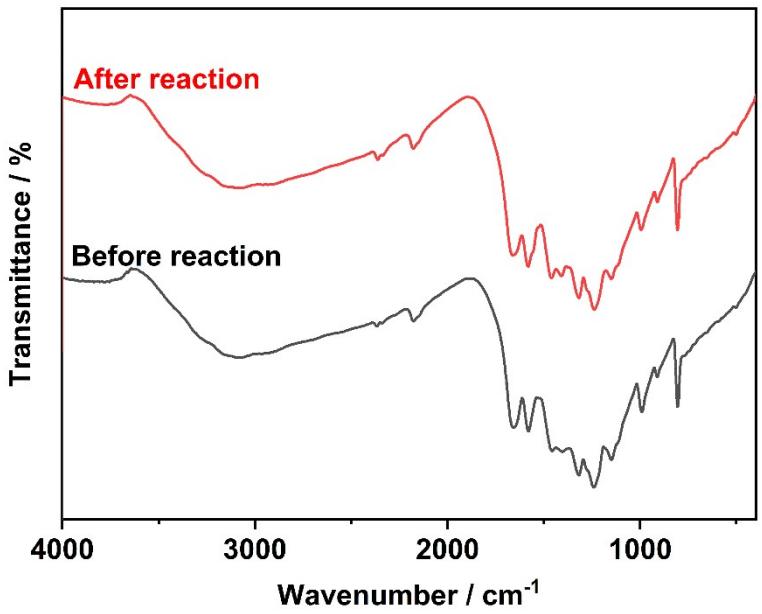

Fig. S14 FTIR spectra of K-PHI before and after the photocatalytic reaction.

Table S3 Comparison of AQE for H_2O_2 production at 420 nm between this work and previous studies.

Photocatalyst	Dosage (mg mL^{-1})	Sacrificial agent	AQE	Ref.
K-PHI	**0.5**	**10% ethanol**	**54.2%**	**This work**
CN-0.3	0.5	10% ethanol	47.1%	S1
CN-K_4Na_2	0.25	25% ethanol	43.7%	S2
CN-K/Na3	0.2	5% isopropanol	23.9%	S3
CN-NH_4-NaK	0.5	10% isopropanol	28.4%	S4
Na-PCN	1	10% ethanol	22.3%	S5
fl-CN-530	0.5	10% ethanol	9.0%	S6
HTCN	0.2	1% isopropanol	21.5%	S7
akut-CN	0.5	10% ethanol	17.2%	S8
CNR	0.4	10% isopropanol	14.58%	S9
PHI-0.5	0.2	5% ethanol	17.8%	S10
O/K-PCN1.6	1	5% ethanol	8.53% [a]	S11
KCMCN	0.4	0.5% isopropanol	7.5%	S12
m-CNNP	1	10% isopropanol	0.55%	S13
ACNN	0.5	10% isopropanol	30.7% [b]	S14

[a] measured at 400 nm. [b] measured at 429 nm.

References

S1 J. Yang, Y. Wang, H. Zhang, L. Shangguan, X. Cao, Y. Guo and J. Sun, *Mater. Today Chem.*, 2025, **49**, 103111.

S2 C. Shi, R. Pan, J. Yuan and C. Liu, *Adv. Funct. Mater.*, 2025, **35**, 2500342.

S3 J. Yue, H. Yang, L. Zhou, C. Liu, S. Wang and X. Kang, *Appl. Catal. B Environ. Energy*, 2025, **361**, 124599.

S4 F. He, Y. Lu, Y. Wu, S. Wang, Y. Zhang, P. Dong, Y. Wang, C. Zhao, S. Wang, J. Zhang and S. Wang, *Adv. Mater.*, 2024, **36**, 2307490.

S5 L. Jian, Y. M. Dong, H. Zhao, C. S. Pan, G. L. Wang and Y. F. Zhu, *Appl. Catal. B: Environ.*, 2024, **342**, 123340.

S6 B. Feng, Y. Liu, K. Wan, S. Zu, Y. Pei, X. Zhang, M. Qiao, H. Li and B. Zong, *Angew. Chem. Int. Ed.*, 2024, **63**, e202401884.

S7 Y. Zhang, Q. Cao, A. Meng, X. Wu, Y. Xiao, C. Su and Q. Zhang, *Adv. Mater.*, 2023, **35**, 2306831.

S8 S. Li, B. Feng, X. Zhang, J. Tian, D. Wang, Y. Pei, M. Qiao, Y. Li and B. Zong, *Appl. Catal. B: Environ.*, 2023, **335**, 122879.

S9 T. Yang, Y. Tang, F. Yang, J. Qu, X. Yang, Y. Cai, F. Du, C. M. Li and J. Hu, *Chem. Eng. J.*, 2023, **475**, 146497.

S10 Z. Yang, L. Li, J. Cui, S. Shao, S. Zeng, K. Wang, D. Ma, C. Hu and Y. Zhao, *Chem. Eur. J.*, 2022, **28**, e202202122.

S11 B. Li, N. Li, Z. Guo, C. Wang, Z. Zhu, X. Tang, G. Andrew Penyikie, X. Wang and P. Huo, *Chem. Eng. J.*, 2024, **491**, 152022.

S12 Q. Cao, X. Wu, Y. Zhang, B. Yang, X. Ma, J. Song and J. Zhang, *J. Catal.*, 2022, **414**, 64-75.

S13 W. Liu, C. Song, M. Kou, Y. Wang, Y. Deng, T. Shimada and L. Ye, *Chem. Eng. J.*, 2021, **425**, 130615.

S14 S. Wu, H. Yu, S. Chen and X. Quan, *ACS Catal.*, 2020, **10**, 14380-14389.